Materials Research Proceedings 54 (2025) 344-353 https://doi.org/10.21741/9781644903599-38

A Preliminary study: Support-free manufacturing of rotationally symmetric pipes from continuous carbon fiber reinforced polymers with multi-axis 3D printing

Zsolt KÁLLAI[1,a] *, Johann KIPPING[1,b], Jan BREMER[2,c] and Thorsten SCHÜPPSTUHL[1,d]

[1]Hamburg University of Technology, Institute of Aircraft Production Technology, Denickestr. 17, 21073 Hamburg, Germany

[2]BCT Steuerungs- und DV-Systeme GmbH, Carlo-Schmid-Allee 3, 44263 Dortmund, Germany

[a]zsolt.kallai@tuhh.de, [b]johann.kipping@tuhh.de, [c]j.bremer@bct-online.de, [d]schueppstuhl@tuhh.de

Keywords: Radial 3D Printing, Continuous Carbon Fiber Reinforced Polymers, Carbon Fiber Pipes

Abstract. This paper presents an innovative approach that combines multi-axis fused filament fabrication (FFF) with continuous carbon fiber reinforced polymers (CFRP) to evaluate the feasibility of manufacturing rotationally symmetric CFRP pipes without mandrels or support structures. Traditional methods, such as filament winding, encounter limitations with geometric complexity and require tooling that makes them unsuitable for producing complex, individual parts. The proposed process uses the manufacturing flexibility of FFF and advantageous material properties of CFRP to create rotationally symmetric pipes on-demand. In this article, the experimental setup is described, the material and process-related challenges are discussed and a preliminary study that involves the printing of rotationally symmetric pipes to verify the viability of the process is presented. The findings aim to advance additive manufacturing techniques, enabling the production of lightweight, customized pipes for various industrial applications, and establishing this method as a cost-effective and efficient alternative.

Introduction

Carbon fiber reinforced polymers (CFRP) are a composite material that reach a very high strength-to-weight-ratio and are one of the most promising materials in the future of lightweight construction [1]. This is achieved through the combination of carbon fibers, which exhibit high stiffness with low weight due to their strong atomic bonding, and a polymer matrix that functions as a binding element, coupling the dry fibers together and enabling a smooth surface finish. The application range of CFRP includes all lightweight and high-performance application scenarios such as sports, aviation and space [2].

With the rise of additive manufacturing (AM) and specifically fused filament fabrication (FFF), this material has long been considered for 3D printing. First in the form of chopped fibers, which can improve certain properties of the printed parts, but do not fully utilize the potential of CFRP [1]. This is why recent research has focused on printing continuous fiber reinforced polymers, which have the added benefit of enabling the orientation of the highly anisotropic extruded material strand according to the load case. Even if a lot of progress has been made in this direction, classical manufacturing processes like tape-laying and hand layup far exceed FFF and other AM methods in achievable quality and mechanical properties [1]. This is mainly due to impregnation issues, missing consolidation, void formation, smaller fiber volume factor and insufficient compaction [1, 2].

Content from this work may be used under the terms of the Creative Commons Attribution 3.0 license. Any further distribution of this work must maintain attribution to the author(s) and the title of the work, journal citation and DOI. Published under license by Materials Research Forum LLC.

For rotationally symmetric parts, the classical manufacturing method is filament winding (FW), where the fiber stock material is wound onto a mandrel. This enables a degree of control over the fiber direction and position and is comparably faster and more flexible than other classical methods [3]. Drawbacks include the necessity to manufacture expensive mandrels and the inability to include undercuts due to the winding nature of the process. Furthermore, non-symmetric components and elliptical or varying cross sections are possible, for example, with robotic filament winding, but are limited, with the process being restricted in possible cross section geometries in general [4, 5].

This work aims to present a concept for combining the advantages of AM and CFRP to yield an equivalent process to filament winding using multi-axis FFF, which additionally can eliminate the geometrical restrictions of classical filament winding. The challenges and requirements are analyzed and a preliminary study is conducted by manufacturing rotationally symmetric pipes to verify the viability of this process.

The proposed method applies compaction normal to the deposited surface, which is not possible in every case with three-axis FFF because the print head orientation must align with the normal direction of the part's cross-sectional area. Furthermore, three-axis FFF requires support structures for overhangs in pipes of varying diameters, where compaction forces partially act towards the removable supports. Eliminating the need for both the expensive mandrel and support structures makes the proposed process, if viable, a highly economical alternative that saves material, costs, and time. Additionally, it drastically increases design freedom by allowing the inclusion of undercuts and complex cross-sectional geometries.

The subsequent section presents the current state of research in CFRP and filament winding, multi-axis printing machines and printing pipes without support material. The printing machine used in this work is described in section Experimental Setup, followed by a discussion of the process and material related challenges and requirements. To assess the viability, the preliminary study is discussed in section Demonstrator and Results.

State of the Art

CFRP and Filament Winding. Filament winding has been a key manufacturing process in the production of composite structures, offering high strength and customizable fiber orientation. Recent advancements in filament winding technology have significantly enhanced its capabilities, particularly through automation and innovative manufacturing techniques.

Carosella et al. provide a comprehensive review of advancements in fiber winding, particularly through the integration of high degrees of freedom (DOF) in robotic systems and the use of additional linear axes. Automation not only improves efficiency but also enhances the quality of the composite by optimizing tensions to improve compaction and fiber volume fraction, reducing porosity and minimizing delaminations. Carosella et al. present three automated processes: classical robotic filament winding, coreless filament winding, and spatial winding. The coreless FW innovatively uses two tools, allowing fibers to be spaced out and layered, while spatial winding uses a robotic setup to interlock fibers, forming a spatial structure [4].

Azeem et al. discuss the application of filament winding in the manufacture of pressure vessels. This involves understanding winding patterns, finite element techniques, and optimization approaches. The focus is on achieving the right balance between structural integrity and material efficiency, which is crucial for the high-pressure environments in which these vessels operate [5].

The pretension force applied to carbon fibers during the FW process is critical. Akkus and Garip investigate the impact of pretension on the tensile strength of continuous carbon fibers. The study found that while pretension helps in the proper laying of fibers on cylindrical pipes, it also induces damage, particularly due to fiber movement through pulleys in the pretension unit [6].

Bodea et al. and Mindermann et al. explore the potential of coreless filament winding. Bodea et al. propose a robotic coreless FW technique primarily for construction, producing hyperboloid

and tubular components. This method requires specialized tools but offers new possibilities in architectural components [7]. Mindermann et al extend this concept to natural fibers, identifying flax as having significant promise, which aligns with the increasing emphasis on sustainable and eco-friendly materials in manufacturing [8].

Jois et al. conduct a systematic analysis of towpreg parameters such as tack, resin content, and width, which are crucial in determining the quality and consistency of the filament winding process. Understanding these parameters allows for better control over the material properties and the final composite structure [9].

Früh and Knippers introduce a multi-stage filament winding process, which enables the creation of complex geometries, including concave cross-sections. This method involves winding a convex geometry and then deforming it post-winding by dissolving soluble mandrels. Despite its potential, this process presents challenges such as the need for complex mandrel shapes and specialized software for soluble mandrel materials, with the limitations of geometry and part quality yet to be fully understood.

In conclusion, the field of filament winding is experiencing rapid advancements through the integration of automation, exploration of new materials, and innovative manufacturing processes. These developments are expanding the applicability of filament winding, enhancing the quality of produced composites, and paving the way for more complex geometries in various industries [3].

Multi-Axis Printing Machines. The term multi-axis printing machine has been used to describe not multiple axes, but any type of printer exceeding the standard amount of three DOF. There exist many different versions of these machines. A clear definition of the solution space and methodic derivation of a machine specifically built for the purpose of small scale FFF of CFRP parts can be found in [10]. The printing machine used in this work is analyzed and described in [11, 12].

Printing Pipes without Support Material. Printing pipes using FFF and CFRP has been proposed before, such as in a preceding publication by the authors of this work [12]. Most of the approaches have the common advantage of removing the necessity of support material [13–15], with some notable exceptions like Zhang et al., where the printing of CFRP is done on hollow forms [16].

Materials

Primary Material. For the printing process, a pre-impregnated, continuous carbon fiber reinforced thermoplastic filament is used. The filament named “Carbon Fiber” is produced by the company Markforged and contains approximately 1000 carbon fibers, along with sizing agent and Polyamide serving as the matrix material [17]. With an outer diameter of around 0.35 mm, the filament requires custom components for printing. Comprehensive details regarding its specifications and recommended application are readily accessible on the Markforged website [18].

Secondary Material. In an experiment described in section Demonstrator and Results, a detachable component is initially printed to provide additional clearance between the print head and the platform, ensuring a collision-free printing process. After printing, this base part is removed and discarded. The material used is "Raise3D Industrial PA12 CF Support Filament", which is compatible with polyamide-based CFRP filaments. This material allows the base to be easily removed from the demonstrator by breaking it off. Further information about this material can be found on the website of the manufacturer [19].

Experimental Setup

Kinematics. The experiments are executed on a dual-robot experimental setup, seen in Fig. 1, which consist of two synchronized 6-axis ABB IRB2600 robots. Robot 1, which carries the print system, is mounted on the platform, while Robot 2, which carries the printing bed, is suspended from an L-shaped beam. The 12-axis setup enables multi-axis 3D printing with enhanced flexibility and can meet the material compaction requirements for executing radial 3D printing

without collisions. For a more detailed description of the experimental setup, including its accuracy and precision, the reader is referred to a prior work [11].

Printing System. The printing system that is mounted onto the flange of Robot 1 consists of two distinct print heads arranged in a rotating tool change system. One is designed for extruding conventional 3D printing material with the standard 1.75 mm filament diameter. The other print head is specialized for printing CFRP filament. Therefore, it is equipped with a dedicated material extruder and a cutter. The hotend is equipped with a Markforged nozzle, which is designed to be used with the Markforged material. It features an additional surface adjacent to the outlet, intended to compact the extruded material onto the preceding layer or starting surface. Moreover, the nozzle is equipped with a PTFE tube that is used for filament guiding.

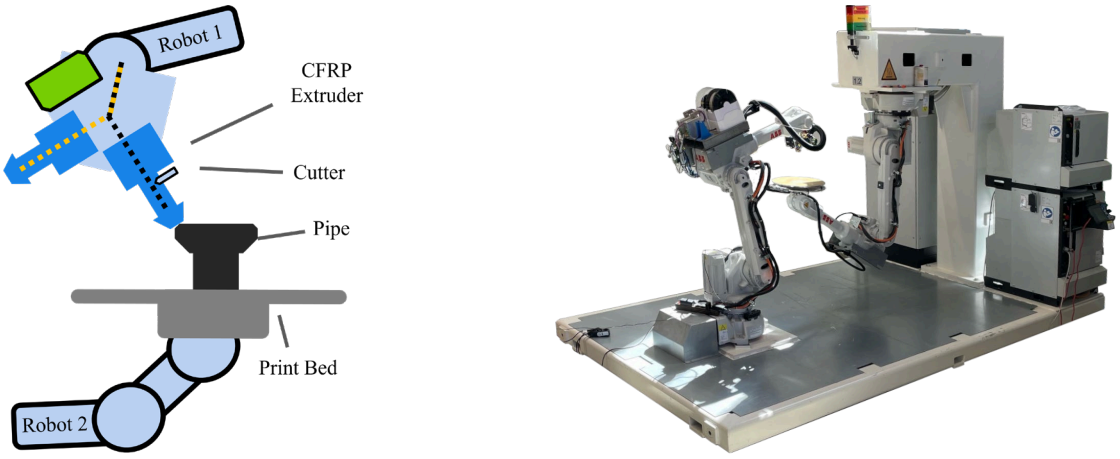

Figure 1 – Left: Schematic representation of the experimental setup with labelled components relevant for radial 3D printing. Right: Dual-robot-based experimental setup employed in this work.

Challenges

Material Requirements. The CFRP filament contains a predetermined number of fibers and matrix material, allowing it to be placed at a constant layer height of 0.125 mm, as specified by the manufacturer. Using a smaller layer height may damage the fibers due to the applied compaction force, potentially reducing the mechanical properties of the finished part. Conversely, selecting a thicker layer height may result in inadequate material compaction, possibly leading to issues with layer bonding.

To create parts suitable for future applications, ensuring proper material compaction is crucial. This should be achieved by maximizing the overlapping surfaces between layers and applying the compaction force onto the already deposited material. With conventional three-axis FFF machines, overhangs in parts with varying cross-sections are formed by stacking dislocated layers, as shown in the middle of Fig. 2. Support structures become necessary when the angle of the overhang exceeds 45 degrees, as the placed layer cannot support itself. This approach reduces the connecting surface area between layers and results in the compaction force partially acting towards the support material, which is removed after printing. Consequently, this is suspected to lead to regions that are not properly compacted, compromising layer adhesion and potentially initiating failure mechanisms. In contrast, the proposed radial printing method, depicted on the right of Fig. 2, applies compaction normal to the surface of the already deposited material, maximizing the connecting surface area between layers and increasing adhesion, without using support structures.

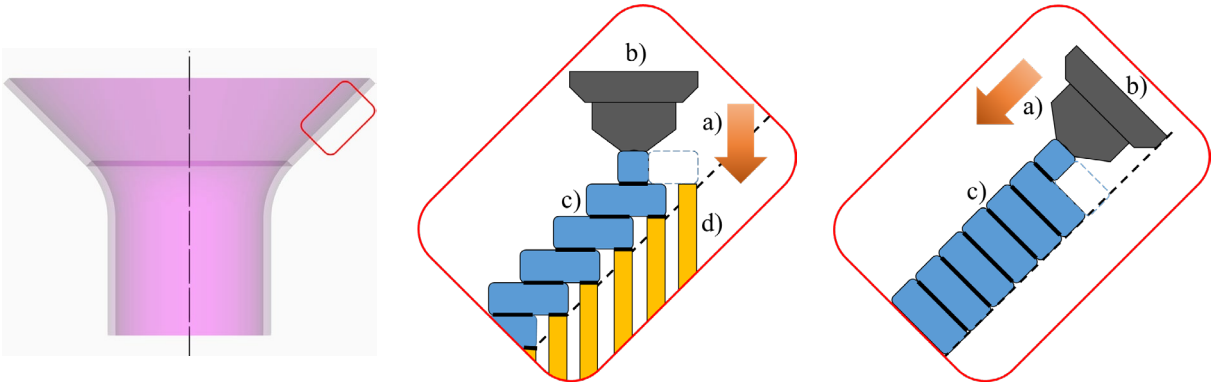

Figure 2 – Left: Rotationally symmetric pipe. Middle: Pipe printed with the conventional printing process where a) direction of the compaction force, b) nozzle, c) printed layers, with bold lines indicating the connecting surface area, d) support structures. Right: Radially printed pipe, where a) direction of the compaction force, b) nozzle, c) printed layers, with bold lines indicating the connecting surface area.

Hardware Challenges. Although the 12-axis experimental setup offers an enhanced manufacturing flexibility, certain hardware restrictions of the robots must still be addressed. Specifically, for safety reasons, the robots' axes are constrained to prevent movement outside their workspace, which is primarily limited to the area above the platform. This restriction reduces the range of axis movements and the number of reachable poses. Additionally, the cabling for the print system and print bed limits axis 6 of each robot from rotating endlessly.

As the system was designed for experimenting with various printing approaches, it is not specifically tailored to the hardware requirements of radial printing. Notably, the print bed is oversized for this process and risks collisions with other hardware components. Furthermore, the print system presents an additional challenge, as the inactive print head rotates with the active one during radial printing, increasing the likelihood of collisions with the print platform or the part. Finally, the geometry of the nozzle and the CFRP print head creates another limitation, as they are not optimized for a narrow clearance angle that is necessary for advanced, collision-free material placement.

Extrusion Control. The current CFRP print head supports two different techniques for filament feeding, a solution developed to synchronize the material placement speed with the speed of the printing robot. Synchronization is a challenge for robot-based 3D printing systems, as maintaining a constant robot speed is difficult, due to varying speeds and accelerations of the different axes to reach the defined pose. The challenge becomes more complex when using continuous CFRP filament, as material placement needs to be precise. If the filament feed rate is slower than the speed of the robot, the designed placement path cannot be maintained. This irregularity can create tension in the material, potentially leading to material breakage and requiring the print to be restarted. Conversely, if the placement speed exceeds the robot's speed, the placed material may become wavy, compromising the mechanical properties of the finished part.

Due to the inability to achieve complete synchronization with the current setup, a workaround was proposed enabling the CFRP filament feed to change between active and passive modes. In active feed mode, the filament is pushed forward by the gears of a specialized extruder. In passive mode, the filament is pulled from the spool by the robot's movement. This method is effective because the continuous fibers in the filament act similar to a rope, where one end adheres to the print surface, holding the material in place, while enough tension is built through the movement of the nozzle to pull the material from the spool into the hotend.

A pneumatic valve was added to the extruder to switch between modes, controlling whether the gears engage with the filament. The printing process begins by actively adhering the filament to

the surface and then switches to passive mode to allow synchronized placement throughout the remainder of the process.

Printing Process

The printing process is presented through the steps of the printing workflow, as shown in Fig. 3, which closely resembles the conventional FFF process. It begins with the design of the workpiece, followed by slicing according to user-defined parameters. After slicing, path-planning is conducted, and the paths are post-processed into RAPID code, which is the programming language of the robotic setup. The resulting program is then simulated in an offline robot programming and simulation software, where the robot poses are verified for reachability, and the paths are adjusted to avoid singularities. Additionally, print paths are checked for clearance to prevent collisions during printing. Once these steps are completed, the modified program blocks are transferred to the controller of the experimental setup, where they can be executed. The following paragraphs provide a detailed description of these steps of the printing process.

Workpiece Design. The process begins with the design of the workpiece to be manufactured. This step, along with the subsequent steps until simulation, is executed in OpenARMS, the framework software of BCT. Within this software, the user can graphically create the workpiece using a user interface (UI) as illustrated in Fig. 3 (top left). Initially, the size of the print area and the position of the workpiece must be defined. Once these parameters are set, the user can create the desired part by adding linear and circular segments. Once the contour of the part is defined, it is rotated around the rotation axis to establish the final geometry, as shown in Fig. 3 (top right).

Slicing. After finalizing the part design, the next step is slicing. The part can be sliced using three different strategies: as discrete slices, as a connected part, where each layer's start- and end point align on a line, or as a continuous part, created as a single spiral path. In addition to selecting a slicing strategy, the user can define parameters such as points per profile, layer height, and settings regarding the contour or the infill patterns. Once these parameters are configured, the slicing process is executed. An example of the slicing method can be seen in Fig. 3 (bottom left).

Path Planning and Post-Processing. The next step is path planning, which starts with defining the lead-in and lead-out paths for fast, rough tool positioning, as well as defining the paths required for material change and travel movements between layers. After these operations are completed, the path planning process continues by creating the movements for the printing process. Once this step if finished, the post-processing phase begins. During this phase, the robot paths and additional movements are converted into an ABB robot program. This program includes all necessary process parameters, such as the amount of material to be extruded and the speed of printing. Upon completion, the operations in OpenARMS are finalized, and the robot program is ready for simulation.

Simulation. To ensure collision-free execution, the created print paths are simulated using an offline robot programming and simulation software. In this software, the generated points of the print paths are evaluated to ensure they are reachable with the tool center point of the print head, and the paths are checked for singularities. If any points are not reachable, they are adjusted to resolve this issue. Additionally, a collision check is performed at this stage to ensure that the robot movements have sufficient clearance between hardware components and the workpiece. If adjustments are required, the paths undergo post-processing again to modify positions or orientations as needed. Furthermore, during this step, the program is divided into manageable blocks. This is necessary because the robot controller can slow down when attempting to load programs with more than 5000 path points. Once these adjustments are complete, the paths are transferred to the robot's controller.

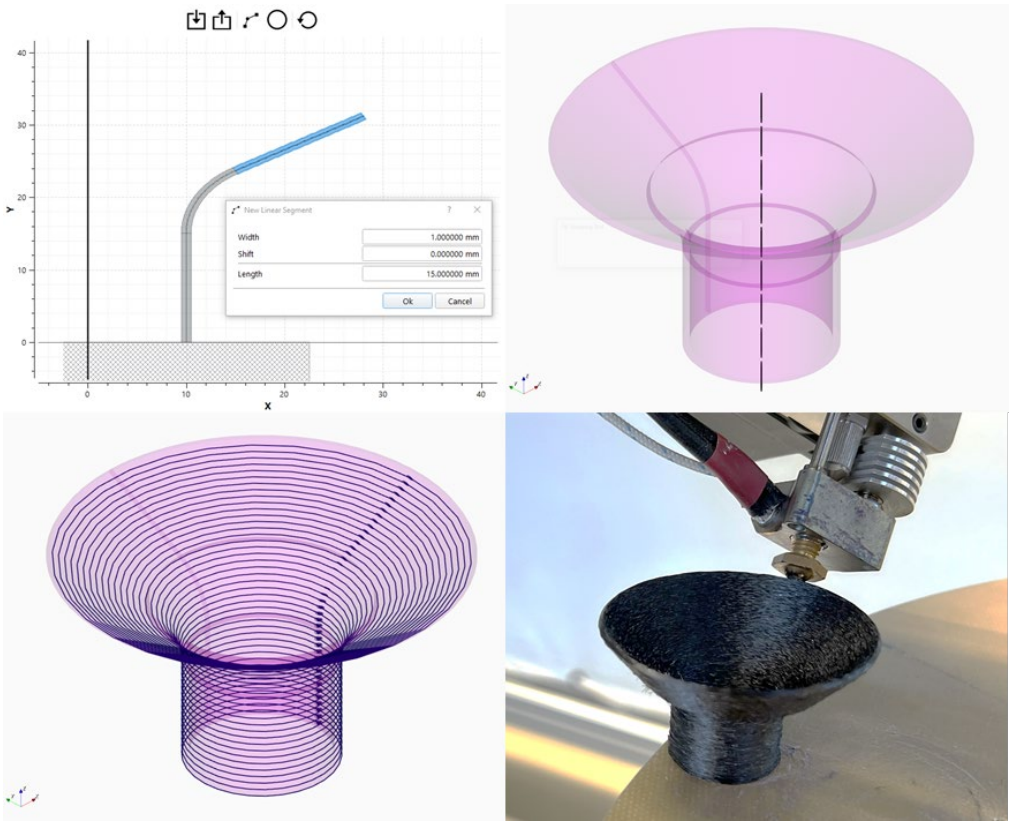

Figure 3 – Top left: User interface of the part design. Top right: Completed design of a rotationally symmetric pipe. Bottom left: Sliced part (layer height adjusted to 1 mm for visibility). Bottom right: Radial 3D printing of a part

Execution. In the final step, the print temperatures are set for the experimental setup, and both the nozzles and the print platform are heated. The programs are executed using a module that automatically loads and unloads the program blocks. Initially, the autoload module loads the first two program blocks and begins executing the first one. Once the first block is completed, execution continues with the second block, during which the controller unloads the first block and loads the third one. This process repeats until the entire program is executed. After printing is finished, the print bed is cooled, and the completed workpiece is removed.

Demonstrator and Results

In this section, the viability of support-free, radial 3D printing with CFRP filament is demonstrated through the manufacturing of three rotationally symmetric pipes. This set of experiments is designed to illustrate that the previously identified challenges can be overcome, confirming the potential of the process for further research.

Part design. The rotationally symmetric pipes used in this demonstration are made of three distinct sections. This elementary design is employed to test the viability of the process. The first section is a 15 mm long straight segment positioned 10 mm away from the rotational axis. This is followed by a 10 mm long curved section with a variable angle of curvature: 20° for the first pipe, 40° for the second, and 60° for the third. The resulting geometries can be seen in the top row of Fig. 4. The curved section serves as a transitional part leading to the third section, which is another 15 mm straight section. Here, the material is placed radially at the defined angle relative to the previous layer. For simplicity, thin-walled pipes are considered for these experiments. Therefore, the wall thickness is set to the minimum width of the CFRP material bead, which is 1 mm.

Slicing. The parts are sliced using a connected layer strategy to ensure smooth transitions between layers, with a layer height of 0.125 mm. As thin-walled parts are printed, only the contour

parameter needs to be adjusted in the UI. Lastly, the number of points per profile is set to 40 to achieve a smooth profile.

Path planning and post-processing. The lead-in/lead-out points are positioned 100 mm away from the start- and end points, while a 100 mm clearance is used for the tool change. With the connected layers strategy, no additional travel movements are necessary. Next, the path planning is executed, and the generated paths are post-processed into robot code.

Simulation. The exported robot codes are transferred into the simulation environment, where they are evaluated for collisions, reachability, and singularities. Since the code for the first pipe involves less complex axis movements, no changes in point orientations are required. However, for the second pipe, point orientations must be adjusted to avoid collisions with the print platform. Printing the third pipe requires a supporting base structure. To achieve this, a 100 mm long straight pipe with a 20 mm diameter is printed using the secondary material. This allows for the collision-free manufacturing of the third pipe. After adjusting the programs, they are divided into smaller blocks.

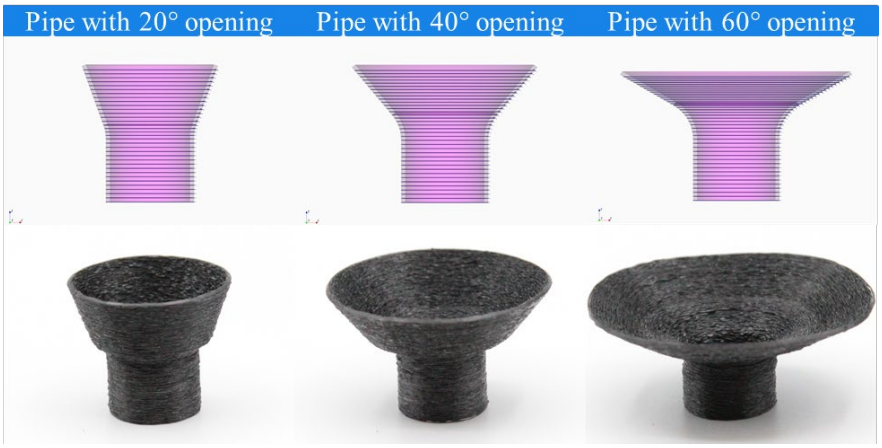

Figure 4 – Top row: Design and slicing of the rotationally symmetric pipes (layer height adjusted to 1 mm for visibility). Bottom row: 3D support-free, rotationally symmetric CFRP pipes

Execution. With the robot codes prepared, the components of the experimental setup are heated to their required temperatures. The CFRP hotend, along with the print head for creating the base part, is heated to 270 °C, while the print bed is set to 60 °C. Subsequently, the program blocks are executed using the autoload function. After finishing the programs, the heat bed is cooled down to remove the finished parts.

Results. The experiments were successfully completed; all pipes were printed without issues. All path points were reachable, and the robot executed the paths without colliding with the workpiece or other hardware components. The printed pipes are displayed in the bottom row of Fig. 4. The first and the second produced parts are complete, with no gaps between the radially placed layers, indicating proper compaction. However, the third part exhibits some gaps between layers. Additionally, the final profile of the third part deviates from its intended form, failing to produce a perfect circle. The second segment of each part also shows unexpected transitions, deviating from the designed geometry.

Discussion and Outlook

The rotationally symmetric pipes were successfully manufactured without support structures with radial 3D printing. The challenges related to material, hardware and process were overcome, demonstrating the feasibility of radial 3D printing with continuous carbon fiber. The presented results could open up possibilities for the automated manufacturing of complex, individual carbon

fiber pipe systems and present a possibility for further process synergies with other composite manufacturing techniques.

However, the process has limitations, as shown by the deviations from the designed form and the appearance of gaps between layers in case of the third part with high wall angle. These issues may originate from positional inaccuracies of the robot and optimization issues from the slicer.

To address these challenges, the printing hardware could be adapted to the process by reducing the print bed size and utilizing a dedicated print head with a narrower clearance angle. Furthermore, optimizing the system to allow continuous rotation of the sixth axis of the suspended robot holding the print bed could enhance the process. This improvement would enable the print platform to manage rotational movements while the print head positions itself along the contour of the part.

The second segment of each part showed deviations from their design as the transition is not smooth as intended. This issue is likely due to the slicer software, which needs optimization to correct tool orientation errors. Furthermore, consideration of active path compensation strategies is necessary, as the filament is extruded not at the center of the nozzle's outlet but on its side, potentially affecting dimensional accuracy. Implementing active material feed with a belt-driven extruder could address this issue, potentially improving path and dimensional accuracy.

Beyond this preliminary study, additional parts with varying angles need to be printed to quantify the reliability and applicability of the process to more complex parts. The quality of the printed parts should be assessed through material tests and microscopic evaluations to verify the quality of compaction in the radial segments. Such a validation can confirm the capabilities of the printing process. Insights gained from this quality assessment could expand the knowledge base of 3D printing with continuous carbon fiber, potentially aiding this process to become a viable manufacturing alternative for complex carbon fiber pipe fabrication.

Acknowledgements
This research was funded by the German Federal Ministry for Economic Affairs and Climate Action (BMWK) through the Federal Aviation Research Program (LuFo VI).

References

[1] Adil, S., Lazoglu, I.: A review on additive manufacturing of carbon fiber-reinforced polymers: Current methods, materials, mechanical properties, applications and challenges. J Appl Polym Sci(7), e53476 (2023). https://doi.org/10.1002/app.53476

[2] Hu, Y., Lin, Y., Yang, L., Wu, S., Tang, D., Yan, C., Shi, Y.: Additive Manufacturing of Carbon Fiber-reinforced Composites: A Review. Applied Composite Materials(2), 353–398 (2024). https://doi.org/10.1007/s10443-023-10178-w

[3] Früh, N., Knippers, J.: Multi-stage filament winding: Integrative design and fabrication method for fibre-reinforced composite components of complex geometries. Composite Structures, 113969 (2021). https://doi.org/10.1016/j.compstruct.2021.113969

[4] Carosella, S., Hügle, S., Helber, F., Middendorf, P.: A short review on recent advances in automated fiber placement and filament winding technologies. Composites Part B: Engineering, 111843 (2024). https://doi.org/10.1016/j.compositesb.2024.111843

[5] Azeem, M., Ya, H.H., Alam, M.A., Kumar, M., Stabla, P., Smolnicki, M., Gemi, L., Khan, R., Ahmed, T., Ma, Q., Sadique, M.R., Mokhtar, A.A., Mustapha, M.: Application of Filament Winding Technology in Composite Pressure Vessels and Challenges: A Review. Journal of Energy Storage, 103468 (2022). https://doi.org/10.1016/j.est.2021.103468

[6] AKKUS, N., Garip, G. E. N. C.: Influence of pretension on mechanical properties of carbon fiber in the filament winding process. The International Journal of Advanced Manufacturing Technology(9), 3583–3589 (2017). https://doi.org/10.1007/s00170-017-0049-z

[7] Bodea, S., Zechmeister, C., Dambrosio, N., Dörstelmann, M., Menges, A.: Robotic coreless filament winding for hyperboloid tubular composite components in construction. Automation in Construction, 103649 (2021). https://doi.org/10.1016/j.autcon.2021.103649

[8] Mindermann, P., Gil Pérez, M., Knippers, J., Gresser, G.T.: Investigation of the Fabrication Suitability, Structural Performance, and Sustainability of Natural Fibers in Coreless Filament Winding. Materials(9) (2022)

[9] Jois, K.C., Mölling, T., Schuster, J., Grigat, N., Gries, T.: Towpreg manufacturing and characterization for filament winding application. Polymer Composites(9), 7893–7905 (2024). https://doi.org/10.1002/pc.28311

[10] Kipping, J., Nettig, D., Kallai, Z., Schueppstuhl, T.: A Robotic Printer for Nonplanar Additive Manufacturing of Carbon Fiber Reinforced Polymers. In: ISR Europe 2023; 56th International Symposium on Robotics, pp. 205–212 (2023)

[11] Kállai, Z., Dammann, M., Schüppstuhl, T.: Operation and experimental evaluation of a 12-axis robot-based setup used for 3D-printing. 52nd International Symposium on Robotics, ISR 2020 (2020)

[12] Kállai, Z., Kipping, J., Schüppstuhl, T. (eds.): Closing the Gap: Exploring Approaches for Printing Lightweight Curved Pipes with Carbon Fiber Reinforced Thermoplastics. The European Society for Composite Materials (ESCM) and the Ecole Centrale de Nantes (2024)

[13] Li, X., Liu, W., Hu, Z., He, C., Ding, J., Chen, W., Wang, S., Dong, W.: Supportless 3D-printing of non-planar thin-walled structures with the multi-axis screw-extrusion additive manufacturing system. Materials & Design, 112860 (2024). https://doi.org/10.1016/j.matdes.2024.112860

[14] Gunpinar, E., Armanfar, A.: Helical5AM: Five-axis parametrized helical additive manufacturing. Journal of Materials Processing Technology, 117565 (2022). https://doi.org/10.1016/j.jmatprotec.2022.117565

[15] Mitropoulou, I., Bernhard, M., Dillenburger, B.: Nonplanar 3D Printing of Bifurcating Forms. 3D Printing and Additive Manufacturing(3), 189–202 (2021). https://doi.org/10.1089/3dp.2021.0023

[16] Zhang, H., Lei, X., Hu, Q., Wu, S., Aburaia, M., Gonzalez-Gutierrez, J., Lammer, H.: Hybrid Printing Method of Polymer and Continuous Fiber-Reinforced Thermoplastic Composites (CFRTPCs) for Pipes through Double-Nozzle Five-Axis Printer. Polymers(4) (2022)

[17] Li, L., Liu, W., Sun, L.: Mechanical characterization of 3D printed continuous carbon fiber reinforced thermoplastic composites. Composites Science and Technology, 109618 (2022). https://doi.org/10.1016/j.compscitech.2022.109618

[18] Markforged. https://markforged.com/. Accessed Last accessed: 4. January 2025

[19] Raise3D. https://www.raise3d.com. Accessed Last accessed: 4. January 2025